IOPscience iopscience.iop.org

Home Search Collections Journals About Contact us My IOPscience

The mechanisms of negative oxygen ion formation from Al-doped ZnO target and the improvements in electrical and optical properties of thin films using off-axis dc magnetron sputtering at low temperature

This article has been downloaded from IOPscience. Please scroll down to see the full text article.

2011 Semicond. Sci. Technol. 26 105022

(http://iopscience.iop.org/0268-1242/26/10/105022)

View the table of contents for this issue, or go to the journal homepage for more

Download details:
IP Address: 115.145.204.84
The article was downloaded on 26/09/2011 at 14:20

Please note that terms and conditions apply.

Semicond. Sci. Technol. **26** (2011) 105022 (7pp) doi:10.1088/0268-1242/26/10/105022

The mechanisms of negative oxygen ion formation from Al-doped ZnO target and the improvements in electrical and optical properties of thin films using off-axis dc magnetron sputtering at low temperature

Huu Chi Nguyen[1], Thanh Thuy Trinh[2,3], Tran Le[1], Cao Vinh Tran[1], Tuan Tran[2], Hyeongsik Park[3], Vinh Ai Dao[2,3,4] and Junsin Yi[3,4]

[1] Faculty of Physics, University of Sciences, Ho Chi Minh City, Vietnam
[2] Faculty of Materials Science, Vietnam National University, Ho Chi Minh City, Vietnam
[3] Information and Communication Device Laboratory, School of Information and Communication Engineering, Sungkyunkwan University, Republic of Korea

E-mail: daovinhai@skku.edu and yi@yurim.skku.ac.kr

Received 13 May 2011, in final form 15 August 2011
Published 26 September 2011
Online at stacks.iop.org/SST/26/105022

Abstract
Transparent conducting aluminum-doped zinc oxide (AZO) films have been prepared on glass substrates by dc magnetron sputtering using ceramic ZnO with 2 wt% Al_2O_3 target. The mechanism of negative oxygen ion generation on an AZO target surface and its influence on the conductivity of films were discussed. The negative ion generation on an AZO target was contributed by the surface ionization leading to the spot emission from Al atoms adsorbed on the AZO target surface. The contribution of negative ions' current was mainly from the erosion area of the target due to its higher temperature. To reduce the damage caused by negative ion bombardment to film growth, an off-axis sputtering system was proposed, where the substrates were placed perpendicular to the target. The effects of distance (d) on the electrical properties of films were experimentally verified in detail. A low resistivity of 3.7×10^{-4} Ω cm, an average transmittance above 85% in the visible range (300–800 nm) and reflectance higher than 85% in the infrared range (2500–4000 nm) were obtained for the films deposited at $d = 2.5$ cm. The overall analysis revealed that the generation of negative ions on the AZO target has a great influence on film growth, especially in the ultra-low pressure deposition process. Our work demonstrates the feasibility of reducing the negative effects of ion bombardment on the quality of films, which would be of great merit for industrial applications.

(Some figures in this article are in colour only in the electronic version)

1. Introduction

Currently, there is great interest in transparent conducting oxides (TCO) for a variety of applications such as solar cells [1], flat panel display [2], organic light-emitting devices [3], surface acoustic wave device [4], piezoelectric transducers [5] and gas sensing devices. In particular, a great deal of research has been carried out on ZnO and conductive aluminum-doped zinc oxide (AZO) thin films due to their advantages over In- and Sn-based TCO films. Undoped and AZO thin films with a high-energy band gap (3.4 eV) exhibit an excellent transmittance in visible light. Besides, ZnO films are especially attractive since they are more cost effective than ITO

[4] Authors to whom any correspondence should be addressed.

 © 2011 IOP Publishing Ltd Printed in the UK & the USA

films and demonstrate higher conductivities and transparencies than the SnO_2-based TCO films.

Many deposition methods have been used to prepare doped and undoped ZnO films. For instance, evaporation [6], chemical vapor deposition (CVD) [7], spray pyrolysis [8] and magnetron sputtering [9] are widely used. Among these methods, magnetron sputtering emerged as a robust method with many advantages such as low substrate temperatures (down to room temperature), good adhesion of films on substrates, superior thickness uniformity and high film density, relatively inexpensive deposition method and scalability to large areas (up to 3–6 m^2) [9].

However, the sputtering method also has some disadvantages caused by the unwanted bombardment on the growing films by negative ions and high-energy neutral atoms. This bombardment has been found from the high resistivity area of thin films [10]. Tominaga *et al* observed that high-energy negative oxygen ions were directly formed on the target corrosion [11]. Part of these ions will be neutralized when passing around the discharge. The bombardment of high-energy oxygen particles on the growing film can vary the properties and structures of films. It has been shown for the ZnO target that the main reason of generating negative ions was the surface ionization of the target surface [12]. The negative ion current emission is mainly caused by the erosion area of the target because of its higher temperature. This phenomenon is ascribed to the film bombardment by energetic oxygen atoms (O atoms), produced by the acceleration of sputtered O^- ions in the cathode fall and their neutralization during transit to the substrate.

In the case of the AZO film deposition process, some studies have already reported about the measurement methods and effect of energetic negative on AZO structure and electrical conductivity. Tsukamoto *et al* [13] reported the observation of the maximum O^- ions flux at the location opposite the erosion track area on the target. They also concluded that the AZO films deposited with the lower O^- bombardment energy showed higher crystallinity and improved the electrical conductivity, which is consistent with Minami *et al* [14]. However, until now the mechanism of negative ion generation on the target has not yet been clearly reported, although information is available regarding the influence of film properties due to the bombardment of negative ion current [12].

In this study, we present the mechanism of generating a negative ion from an AZO target during the sputtering process based on the results published in [15]. Further, to minimize damage due to the bombardment on the growing film surface by negative ions, the reactive gases, substrate temperature, working pressure and distance (d) between the center of target and substrate were adjusted to obtain an optimized condition by using off-axis dc magnetron sputtering.

2. Experimental details

Typically, low conductivity is exhibited by the films that are bombarded by the accelerated sputtered O^- ions in the cathode fall [10]. To reduce the damage caused by the negative ion bombardment on the growing film surface, we propose to use the off-axis system, where the substrates are placed perpendicular to the target to prevent the negative ion current from directly bombarding the film's surface. In this sputtered configuration, the angular distribution of the deposition rate follows the equation: $f(\theta) = a\cos\theta + \cos^3\theta\ (a = -0.8)$. [16]. From this distribution, in this study we used the angular direction for maximum deposition rate of around 30–40°, which agreed with other reports [17].

Figure 1 exhibits a block diagram of our off-axis sputter chamber with three substrate positions of X_a, X_b and X_c, respectively. The substrates placed at X_a and X_b are opposite the target center and the erosion track, respectively, and parallel with the target. The erosion track areas are produced due to the strong magnetic field on the target. At X_c, the substrate can move perpendicular to the target. The distance d, which is defined as the distance from the center of erosion area on the target to the substrate, was adjusted to obtain an optimized deposition condition. h was the height from the target to the center of the substrate and was kept fixed during the film deposition in such a way that the angular distribution of the sputter deposition was around 30–40°.

The AZO thin films were prepared using a ZnO ceramic target doped with 2 wt% Al_2O_3 (7 × 7 cm^2 in dimension). The working pressure of argon (99.5%) reactive gas was varied from 1 to 9 mTorr, keeping the sputtering power and current at 60 W and 0.2 A, respectively. Prior to deposition, pre-sputtering was performed for 10 min to remove any contamination on the target surface. The glass substrates (2 × 2 cm^2) were ultrasonically cleaned sequentially by using acetone, isopropyl alcohol and distilled water for 10 min each. Finally, the substrates were dried at 150 °C to remove the remaining water vapor on the surface. For film deposition, the cleaned-glass substrate was placed at the substrate heater, as is shown in figure 1. The deposition rate throughout the process was approximately maintained in the range 20–30 nm min^{-1}. The substrate temperature was varied from 120 to 280 °C.

The optical transmission spectra of the deposited films were measured by the UV–Vis V-350 spectrophotometer in the wavelength range of 300–1100 nm, and the optical reflectance spectra were measured by FTIR Bruker Uquinox 55 in the wavelength range of 660–25 000 nm. We also present a correlation between the optical and electrical properties of AZO films from which the carrier concentration was determined using the plasma wavelength λ_P value [18]. The sheet resistances of the films were measured according to the four-point probe method. All AZO films were fixed at the same thickness.

3. Results and discussion

3.1. Mechanism of negative ion generation from the AZO target during sputtering

ZnO is a II–VI compound semiconductor whose ionicity resides at the borderline between covalent and ionic semiconductor. The difference in ion radius between Al^{3+}

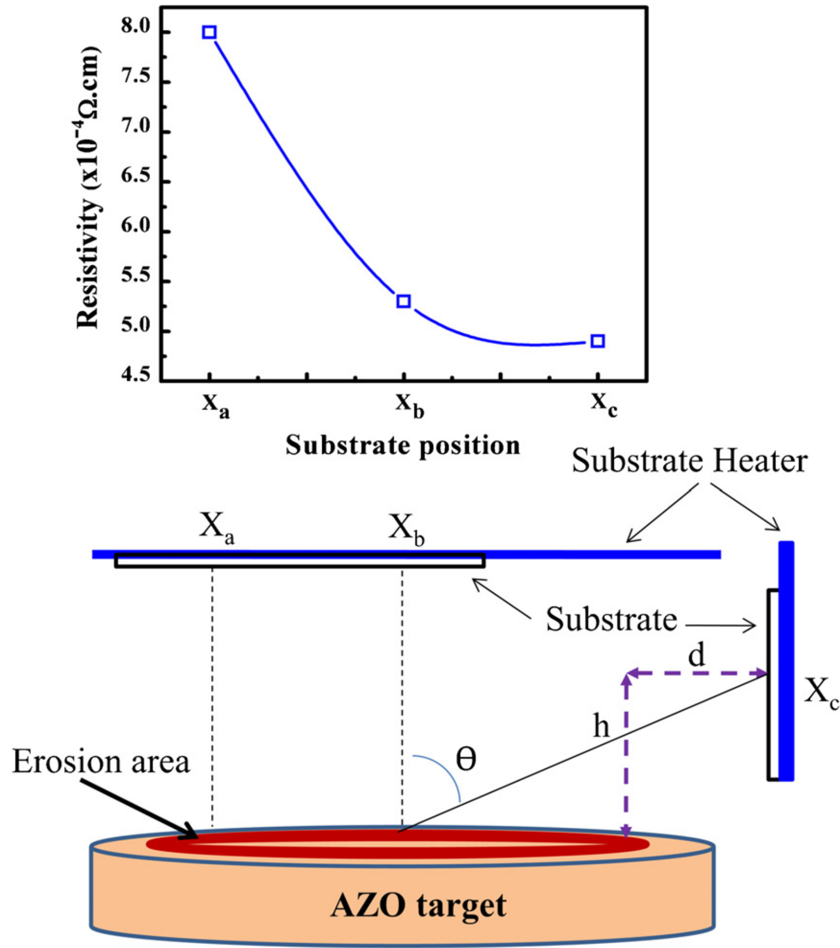

Figure 1. Schematic diagram of the sputtering chamber with off-axis configuration.

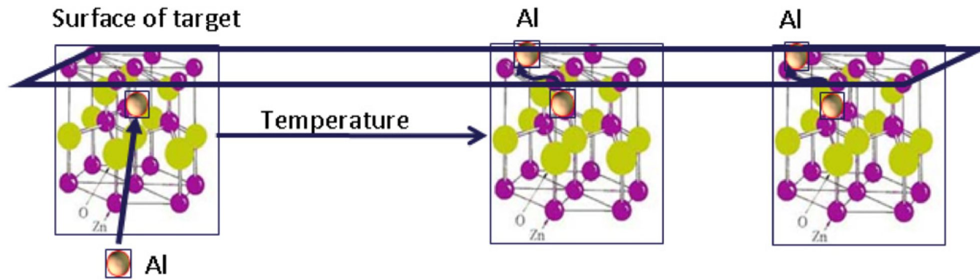

Figure 2. The diffusion process of Al atoms in the ZnO lattice of the AZO target at high temperature.

(0.039 nm) and Zn^{2+} (0.06 nm) would lead to the AZO lattice distortion when Al is incorporated into ZnO lattice [19]. Al ions mostly exist in the form of interstitial precipitation at the grain boundary of ZnO lattice. Besides, the ratio between Al and ZnO atomic radius ($r_{\mathrm{Al}}/r_{\mathrm{ZnO}} = 1.18$ Å/1.625 Å $= 0.726$) shows that Al is easily interstitial solubilized in ZnO octahedral site (the maximum value for this process is 0.732) [20]. At high temperatures (as shown in figure 2), Al atoms easily diffuse to the target surface by overcoming the potential barrier height of the nearest-neighbor particle. The diffusion coefficient of Al dopant follows the equation

$$D = va^2 \exp\left(-\frac{E_D}{KT}\right) \qquad (1)$$

where v is the oscillation frequency of lattice atoms ($\sim 10^{13}$ s^{-1}), a is the lattice constant ($\sim 10^{-8}$ cm), K is Boltzmann's constant and E_D is the potential barrier of the nearest-neighbor particle.

Most Al atoms diffuse along the crystal lattice, especially along the lattice mismatch and through the grain boundary where the diffusion coefficient is larger than that in bulk. Subsequently, Al atoms accumulate at the surface of the target as if they were absorbed by the surface. Consequently, the AZO target's surface becomes chemically inhomogeneous and the emission process of oxygen negative ions on the target surface is mainly at the spots that have a work function value of φ_λ. Based on Langmuir's emission theory [21], particles

that are unevenly distributed on the surface of the cathode with cover order $\theta < 1$ would precipitate in the small spots. The spot emission also occurs on the polycrystalline-target's surface where the work function is different at different lattice planes.

Assuming that the spots distributed on the target's surface have various work function values called $(f_\lambda, \varphi_\lambda)$ and satisfying the condition $(\varphi_{\lambda_{\min}} - S - \sqrt{eE}) \gg KT$, the current density of a negative ion from spot emission is given by the equation

$$i_- = e\bar{A}\exp\left\{\frac{e(S+\sqrt{eE}-\bar{\varphi})}{KT}\right\}$$
$$\bar{A} = NA\sum_\lambda f_\lambda \exp\left\{\frac{e(\bar{\varphi}-\varphi_\lambda)}{KT}\right\}, \tag{2}$$

where S is the electron affinity of oxygen, $\bar{\varphi}$ is the mean work function, E is the electric field, f_λ is the dimension of spot and $\varphi_{\lambda\min}$ is the minimum work function value of the spot emission. Equation (2) suggests that the emission of negative ions does not take place everywhere on the surface; rather, it mainly occurs at the corrosion of the target, where the temperature is highest. Negative ions emitting from the corrosion will be accelerated by the cathode fall and neutralized while moving toward the substrate. These negative ions will bombard the films and lead to a dramatic decrease in the conductivity of the films [10].

Equation (2) indicates that there are two main factors that affect the current density of negative ions from the spot emission. One is the higher temperature in the emission area, which will lead to a higher current density of the negative ion from the spot emission. Thus, a higher current density of a negative ion will originate from the erosion area that has higher temperature than elsewhere on the target's surface due to the collision between the particles and the surface. Another parameter that also affects the conductivity of films is the work function of the metal $\bar{\varphi}$. The lower the metal work function, the higher will be the current density which is consistent with other reports [22].

3.2. Structure and compressive residual stress in films

First of all, so as to demonstrate the efficiency of off-axis configuration, we compared the electrical properties of AZO samples fabricated at X_a, X_b and X_c positions with same sputtered conditions. Note that X_c was located outside the erosion track area with $d = 2.5$ cm and $h = 3.5$ cm. The distance between target and X_a, X_b was 9 cm. The resistivity of AZO films at different positions is presented in the inset of figure 1. While the sample in front of the erosion track shows the highest resistivity of 8.0×10^{-4} Ω cm, the samples placed at the center of the AZO target and perpendicular to the target express the low resistivity of 5.3×10^{-4} and 4.9×10^{-4} Ω cm, respectively. This result has good agreement with other reports regarding the conductivity of TCO versus positions [23]. As described above, the sample placed in front of the erosion track area (X_a) has been bombarded by the negative energetic oxygen ion that causes the degradation in the conductivity. Apart from the erosion area, the sample

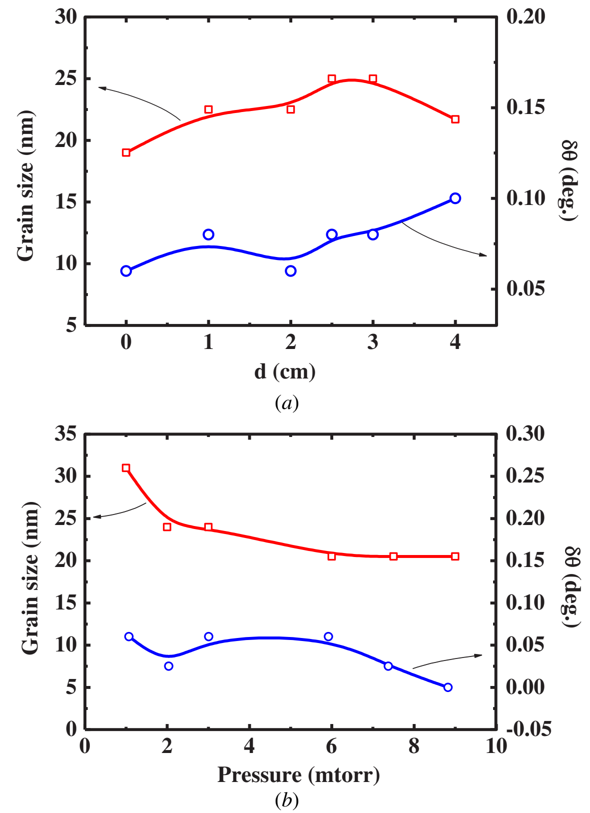

Figure 3. (*a*) Grain size and shift angle versus distance d (at substrate temperature of 120 °C and working pressure of 3 mTorr). (*b*) Grain size and shift angle as a function of working pressure (at substrate temperature of 120 °C and $d = 2.5$ cm).

was less bombarded by the unwanted ions resulting in the improvement in electrical properties. The sample placed in X_c shows a best conductivity implying that the bombardment of the negative ion on the film surface can be reduced effectively by setting the substrate perpendicular to the target (which was called off-axis). With this result, all the following studies in this report have been performed with off-axis configuration.

In order to estimate the effect of bombardment of negative ions on the structure of films, the internal stress of AZO films was estimated using the XRD results (XRD patterns were not shown in this study). Note that all films fabricated in this study oriented along the c-axis which is perpendicular to the substrates. Figure 3(*a*) presents the calculated grain size and $\delta\theta$ from the XRD of AZO thin film as a function of d at a substrate temperature and working pressure of 120 °C and 3 mTorr, respectively. $\delta\theta = \theta - \theta_o$, where θ and θ_o are the diffraction angles from the XRD of thin films and reference ZnO bulk, respectively. Similarly, figure 3(*b*) depicts the grain size and $\delta\theta$ values as a function of working pressure. The compressive residual stress in the AZO thin films was determined using equation [24]

$$\sigma_f = \frac{Y}{2\eta}\frac{\delta\theta}{\tan\theta} \tag{3}$$

where σ_f is the stress of thin films, Y is the Young modulus and η is the Poisson coefficient. In equation (3), Y and η can

be considered as constants since the same material, AZO, was used in our study. Hence, $\delta\theta$ gives a measure of σ_f of the thin films.

Figures 3(*a*) and (*b*) show that the compressive stress of the films does not significantly change with the variations in pressure and distance *d*. The stress occurring in the films is mainly due to the damage caused by the bombardment of unexpected negative ion on the films. As reported in [25], the stresses for AZO films should be mainly attributed to the bombardment by negative ions such as O^-, $O_2{}^-$, AlO^-, $AlO_2{}^-$, $AlO_3{}^-$, ZnO^-, $ZnO_2{}^-$ etc. It is noted that with the off-axis configuration, the films can avoid the direct bombardment of high-energy negative ions on the surface so that the bombardment is considerably reduced and can be negligible. Figure 3(*a*) shows that the grain sizes of films vary in the small range (18–25 nm), with the smallest grain size obtained at the center of erosion ($d = 0$ cm) and the highest value is attained when *d* is around 2.5–3 cm. This perhaps indicates that in this *d* range, the AZO thin films are mostly bombarded by the positive ions. The smallest grain size was achieved at the center of erosion indicating that the negative ion bombardment still has a small effect on the quality of films. As shown in figure 3(*b*), the AZO grain size is slightly reduced with increasing working pressure. The highest value of grain size, 31 nm, was achieved from the sample fabricated at 1 mTorr. The lower the working pressure, the greater the ion bombardment process, so that the ion energy can be conserved when falling in the plasma region and then transmit the total energy to the particles.

It is expected that, in our case, the carrier mobility may not be a factor influencing the electrical properties of the AZO films because the small variations in grain sizes (figure 3) in the film may not lead to pronounced grain boundary scattering effects. Hence, probably only the carrier concentration would affect the electrical property of AZO films.

3.3. Optical and electrical properties of films

The influence of distance *d* and substrate temperature as well as the working pressure on the resistivity and carrier concentration of the films will be discussed in detail. Also, a correlation between the optical and electrical properties will be presented so as to calculate the carrier concentration according to the Drude theory. The transmittance and reflectance spectrum of AZO thin films deposited at a substrate temperature of 160 °C, working pressure of 3 mTorr and the distance $d = 2.5$ cm are shown in figure 4. It can be observed that the average transmission in the visible range (300–800 nm) and the reflection in the infrared range (2500–4000 nm) are above 85%.

From the basic equations, $\tilde{n} = n + i\kappa$ and $\tilde{\epsilon} = \varepsilon' + i\varepsilon'' = \tilde{n}^2$ (ε' and ε'' are the real and imaginary parts of the complex dielectric function ε; n and κ are the real and imaginary parts of the complex index of refraction $\tilde{n}$); a relation between the dielectric function and photo-energy can be derived by applying the Drude theory, which describes the free electron

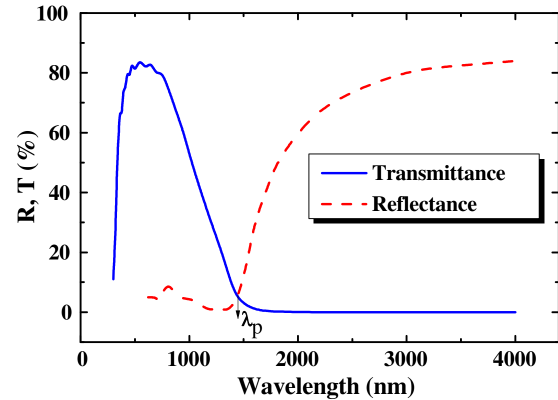

Figure 4. Representative transmittance and reflectance spectra of AZO thin films. λ_P is used to calculate the carrier concentration.

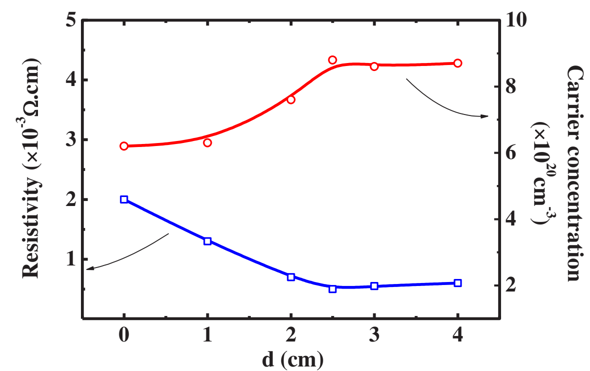

Figure 5. Resistivity and carrier concentration versus distance (at substrate temperature, working pressure, and sputtering power of 120 °C, 3 mTorr, and 60 W, respectively).

contribution to the dielectric function as follows [26]:

$$\varepsilon'(\omega) = \varepsilon_\infty - \left[\frac{\omega_P^2}{(\omega^2 + \gamma^2)}\right] = n^2 - \kappa^2$$
$$\varepsilon''(\omega) = \left(\frac{\gamma}{\omega}\right)\left[\frac{\omega_P^2}{\omega^2 + \gamma^2}\right] = 2n\kappa, \quad (4)$$

where ε_∞ is the residual dielectric constant extrapolated toward high energy ($\varepsilon_\infty \approx 4.5$ [27] in the AZO case), ω is the photon energy, ω_P is the plasma frequency and γ is a collision frequency or the frequency at which the free carries are scattered. The carrier concentration n_e of the AZO film can then be obtained by substituting for the effective electron mass m_c^* of the carriers in the conduction band and plasma frequency ω_P as follows [27]:

$$n_e = \frac{\varepsilon_o m_c^* \omega_P^2}{e^2}, \quad (5)$$

where $\varepsilon_o = 8.854 \times 10^{-14}$ F cm^{-1} is the free-space permittivity; $\omega_P = 2\pi c/\lambda_P$, where λ_P is the plasma wavelength of films determined from the intersection of the transmittance and reflectance spectra. From figure 4, the plasma wavelength of films deposited at substrate temperature, working pressure and *d* of 160 °C, 3 mTorr and 2.5 cm, respectively, is around 1.5 μm.

The resistivity and estimated carrier concentration (from equation (5)) of AZO films, as a function of distance *d*, are

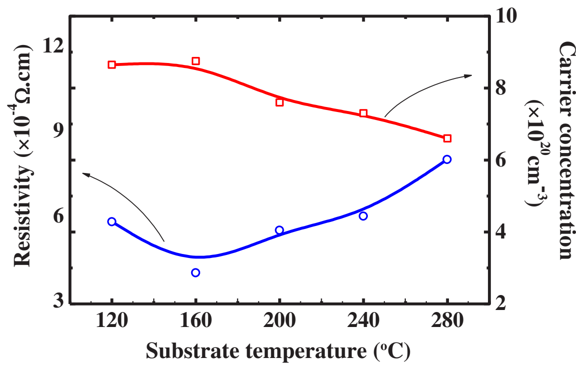

Figure 6. Resistivity and carrier concentration as a function of substrate temperature (at working pressure and distance d of 3 mTorr and 2.5 cm, respectively).

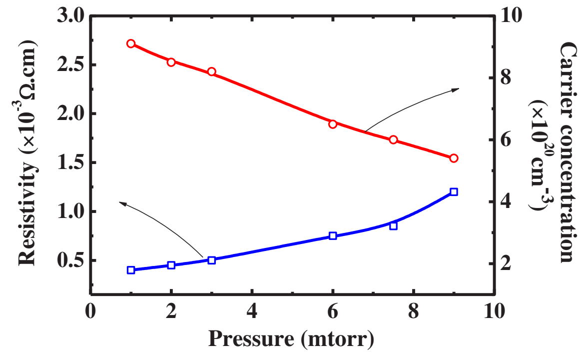

Figure 7. Resistivity and carrier concentration versus pressure (at substrate temperature of 160 °C and $d = 2.5$ cm).

shown in figure 5. In this case, the substrate temperature, chamber pressure, and sputtering power were maintained at 120 °C, 3 mTorr and 60 W, respectively. The figure indicates that the lowest carrier concentration was obtained for the sample fabricated at the center of erosion area at $d = 0$ cm and then increases with increasing d to 2.5 cm. At the center and near the erosion area, resistivity was also observed to be higher than others. It is obvious that the negative ion bombardment still affects the samples kept perpendicular at the center of the erosion area. At $d = 2.5$ cm, the highest carrier concentration of 8.8×10^{20} cm^{-3} and the lowest resistivity of 4.3×10^{-4} Ω cm were achieved. This is due to the fact that at low distance $d = 2.5$ cm, the energetic sputtered particles can reach the films without being scattered or with the least scattering so that the energy is relatively high. In contrast, the carrier concentration of the film slightly decreased with increasing the d value above 2.5 cm. This could be due to the fact that distance d is now probably higher than the mean free path length of the sputtered particles so that these particles collide with one another before arriving at the substrate, and the films did not receive all their energies [28]. Figure 5 also indicates that the resistivity of films decreases when d varies from 0 to 2.5 cm and then shows an increasing behavior upon further increasing the d value. A low resistivity value, 4.3×10^{-4} Ω cm, was obtained for $d =$ 2.5 cm. Repeated experiments showed the same trend.

Figure 6 shows the variations of resistivity and carrier concentration of the AZO film for different substrate temperatures from 120 to 280 °C at a working pressure of 3 mTorr and d of 2.5 cm. As the temperature increases from 120 to 160 °C, the resistivity decreases from 5.8×10^{-4} Ω cm to a minimum value of about 4×10^{-4} Ω cm and then increases upon increasing the substrate temperature. At the substrate temperature of 280 °C, the resistivity is 8.0×10^{-4} Ω cm. The resistivity ρ is proportional to the reciprocal of the product of the carrier concentration n_e and mobility μ. In our study, the change in resistivity with substrate temperature can be mostly ascribed to the change in n_e since the carrier mobility may not be a factor influencing the resistivity as mentioned earlier. It can be seen from figure 6 that the carrier concentration of films increases up to 160 °C and then gradually decreases as the temperature raises to 280 °C. The lowest resistivity of 4.0×10^{-4} Ω cm and the highest carrier concentration of 8.5×10^{20} cm^{-3} were obtained for the films deposited at 160 °C. This result is in good agreement with earlier reports [29].

Generally, the effect of substrate temperature on resistivity and carrier concentration was explained based on the improvement of crystallinity and the decrease of defects [30]. Further, in those reports, the authors employed the on-axis system for the deposition of films and the best conductivity was reported at around a substrate temperature of 250 °C. However, in this study, a high conductivity was achieved at a lower temperature of 160 °C, which cannot be clearly explained by the above reported phenomena. Our results may be explained based on the adsorption process of oxygen atoms on the surface of AZO films. The adsorption of oxygen atoms and formation of O^- ions on the surfaces of films as well as in the grain boundary increases, especially above 160 °C [31]. Each oxygen atom in the AZO film surface can trap two electrons leading to a decrease in carrier concentration, i.e. the resistivity increases as shown in figure 6. Meanwhile, the adsorbed oxygen in the form of O_2^- ions mainly appears at temperatures below 160 °C [31], and thus captures only one electron. However, at temperatures lower than 160 °C, the Al atoms adsorbed on the surface may not have enough kinetic energy to diffuse into the lattice of ZnO in order to interstitial to the Zn site. This resulting in the lower AZO films' carrier concentration compares with the ones at higher sputtered temperature than 160 °C. In conclusion, at 160°C substrate temperature, the sample obtains the lowest resistivity of 4.0×10^{-4} Ω cm.

Figure 7 shows the carrier concentration and resistivity of films as a function of working pressure at a substrate temperature of 160 °C, and $d = 2.5$ cm. The figure demonstrates that as the working pressure increases, the resistivity increases, whereas the carrier concentration calculated from the optical transmittance decreases. The lowest resistivity of 3.7×10^{-4} Ω cm and the highest carrier concentration of 9×10^{20} cm^{-3} were obtained for the films deposited at a working pressure of 1 mTorr. The reduction in conductivity of AZO films at high working pressure can be explained as follows. As the working pressure increases, the mean free path of energetic sputtered atoms emanating from the target is reduced. Meanwhile, the sputtered atoms and argon ions in the chamber collide more frequently, which

can result in the reduction of sputtered atoms energy while traveling to the substrate. Hence, the energetic sputtered particles arrive at the substrate with less kinetic energy, so that Al atoms adsorbed on the surfaces of AZO films may not receive enough energy from these sputtered particles. Due to the low energy received, the mobility of Al atoms would be too low to diffuse into the films in order to enhance the carrier concentration. Thus, our study demonstrates that the optimal conditions for preparing suitable AZO thin films with a low resistivity of $3.7 \times 10^{-4}\ \Omega$ cm and a high concentration of 9×10^{20} cm^{-3} are 1 mTorr Ar pressure, 160 °C substrate temperature and 2.5 cm distance. The experiments were repeated to verify their reproducibility; the trend was observed to be the same.

4. Conclusion

Optimized AZO thin films were prepared using off-axis magnetron dc sputtering, at a distance d of 2.5 cm, low substrate temperature of 160 °C and working pressure of 1 mTorr. The lowest resistivity of $3.7 \times 10^{-4}\ \Omega$ cm, highest carrier concentration of 9×10^{20} cm^{-3} and an average transmission above 85% in the visible range (300–800 nm) were obtained. These better results, especially the low resistivity values, can be attributed to the reduction in the negative ion bombardment emitted from the target surface. The negative ion generation from the AZO target was due to the surface ionization that was formed by the surface absorption of Al atoms on the AZO target surface. The use of off-axis sputter configuration to reduce the negative ion bombardment effect may be easily adapted for the mass production of AZO films with better characteristic properties, especially for low-temperature application.

Acknowledgment

This work was supported by the New and Renewable Energy of the Korea Institute of Energy Technology Evaluation and Planning (KETEP) grant funded by the Ministry of Knowledge Economy, Korean Government, under grant no. 2008-N-PV12-P-02-2-200.

References

[1] Krasnov A 2010 *Sol. Energy Mater. Sol. Cells* **94** 1648

[2] Tominaga K, Iwamura S, Shintani Y and Tada O 1982 *Japan. J. Appl. Phys.* **21** 688–95

[3] Meyer J, Görrn P, Hamwi S, Johannes H H, Riedl T and Kowalsky W 2008 *Appl. Phys. Lett.* **93** 073308

[4] Suchand Sandeep C S, Philip R., Satheeshkumar R and Kumar V 2006 *Appl. Phys. Lett.* **89** 063102

[5] Kakeno T, Sakai K, Komaki H, Yoshino K, Sakemi H, Awai K, Yamamoto T and Ikari T 2005 *Mater. Sci. Eng.* B **118** 70–3

[6] Rusu G G, Râmbu A P, Buta V E, Dobromir M, Luca D and Rusu M 2010 *Mater. Chem. Phys.* **123** 314–21

[7] Kim D Y, Yun I G and Kim H Y 2010 *Curr. Appl. Phys.* **10** S459–62

[8] Kang D W, Kuk S H, Ji K S, Lee H M and Han M K 2011 *Sol. Energy Mater. Sol. Cells* **95** 138–41

[9] Ellmer K 2000 *J. Phys. D: Appl. Phys.* **33** R17–32

[10] Hirata G A, McKittrick J, Siqueiros J, Lopez O A, Cheeks T, Contreras O and Yi J Y 1996 *J. Vac. Sci. Technol.* A **14** 791

[11] Tominaga K, Iwamura S, Shintani Y and Tada O 1982 *Japan. J. Appl. Phys.* **21** 688–95

[12] Tominaga K, Yuasa T, Kume M and Tada O 1985 *Japan. J. Appl. Phys.* **24** 944–9

[13] Tsukamoto N, Wantanabe D, Saito M, Sato Y, Oka N and Shigesato Y 2010 *J. Vac. Sci. Technol.* A **28** 846–50

[14] Minami T, Miyata T and Yamamoto T 2000 *J. Vac. Sci. Technol.* A **18** 1584

[15] Dao V A, Le T, Tran T, Nguyen H C, Kim K H, Lee J H, Jung S W, Lakshminarayan N and Yi J S 2009 *J. Electroceram.* **23** 356–60

[16] Yamamura Y, Takiguchi T and Ishida M 1991 *Radiat. Eff. Defects Solids* **118** 237

[17] Lee Y E, Kim S G, Kim Y J and Kim H J 1997 *J. Vac. Sci. Technol.* A **15** 1194–9

[18] Biswas P K, De A, Pramanik N C, Chakraborty P K, Ortner K, Hock V and Korder S 2003 *Mater. Lett.* **57** 2326–32

[19] Dutta M, Ghosh T and Basak D 2009 *J. Electron. Mater.* **38** 2335–42

[20] Schaffer J P 1999 *The Science and Design of Engineering Materials* 2nd ed (New York: McGraw-Hill)

[21] Langmuir I 1923 *Phys. Rev.* **2** 419

[22] Minami T 2000 *Thin Solid Films* **366** 63–8

[23] Minami T 2008 *Thin Solid Films* **516** 5822–8

[24] Hinze J and Ellmer K 2000 *J. Appl. Phys.* **88** 2443–50

[25] Ito N, Oka N, Sato Y and Shigesato Y 2010 *Japan. J. Appl. Phys.* **49** 071103

[26] Bass M 1995 *Handbook of Optics* (New York: McGraw-Hill)

[27] Qu Y, Gessert T A, Ramathan K, Dhere R G, Noufi R and Coutts T J 1993 *J. Vac. Sci. Technol.* A **11** 996–1000

[28] Dao V A, Choi H W, Heo J K, Park H S, Yoon K C, Lee Y S, Kim Y K, Lakshminarayan N and Yi J.S 2010 *Curr. Appl. Phys.* **10** S506–9

[29] Jayaraj M K, Antony A and Ramachandran M 2002 *Bull. Mater. Sci.* **25** 227–30

[30] Chen M, Pei Z L, Wang X, Sun C and Wen L S 2001 *J. Mater. Res.* **16** 2118–23

[31] Lawless K R 1974 *Rep. Prog. Phys.* **37** 231–316